IEEE Instrumentation and Measurement
Technology Conference
Anchorage, AK, USA, 21–23 May 2002

Corrosion Signal Processing Using Wavelet Analysis and Nyquist Diagrams

Alexander M. Lowe
School of Applied Chemistry, Curtin University of Technology, PO Box U 1987, Perth, Western Australia 6845.
Phone: +61 8 9266 7227, email: A.Lowe@exchange.curtin.edu.au

Halit Eren
School of Electrical and Computer Engineering.
Phone: +61 8 9266 2600, email: h.eren@ece.curtin.edu.au

Abstract *– Electrochemical noise (EN) analysis is a technique that can be used for monitoring corrosion processes. It is often used to obtain information relating to the rate of corrosion by use of the noise resistance and spectral noise impedance calculations. This paper demonstrates two signal processing techniques that can be applied to EN data. An example of a continuous wavelet transform of EN data obtained from a non-stationary system is given. Impedance information is extracted from wavelet transform data and compared with impedance measurements using an independent technique. The complex noise impedance, a novel EN analysis technique developed to compliment the spectral noise impedance, is also described.*

Keywords *– electrochemical noise, wavelet transform, noise resistance, spectral noise impedance, complex noise impedance*

I. INTRODUCTION

Electrochemical noise (EN) [1] refers to the potential and current fluctuations that are measurable on a corroding metal (electrode). In aqueous solutions, the potential noise (EPN) is measured with respect to the bulk solution and the current noise (ECN) is measured between the electrode and an external source such as a potentiostat or another electrode.

Once a set of EN measurements have been obtained, various signal processing techniques can be applied to obtain information about the processes occurring. Typical analyses include the noise resistance [2] [3] [4] and the spectral noise impedance [5] [3].

The noise resistance and spectral noise impedance are obtained from a simultaneous EPN and ECN measurement, as first described by Eden *et al* [2]. A pair of nominally identical electrodes are electrically coupled and the EPN at the point of coupling is logged with respect to a reference electrode. Simultaneously, the ECN flowing between the two electrodes is logged.

The spectral noise impedance has been theoretically [3] and experimentally [6] [7] linked to the equivalent electrochemical impedance of the corroding metal. This impedance (in particular the magnitude at low frequencies) can be used to infer information regarding the rate of corrosion [8] [9] [7].

An alternative, non-EN, method for measuring the low frequency magnitude is the so called linear polarization (LP) technique [10]. The results from LP and spectral noise impedance calculations can be compared to help validate results.

The wavelet transform has also attracted interest for analysis of EN [11], particularly for detecting the onset of localized corrosion. It has the advantage of being a time varying frequency analysis and so may be useful for studying dynamic systems.

In the first part, this paper will demonstrate an example continuous wavelet transform of an EN signal under non-stationary conditions to show how it can provide time varying information. Further example will be given to show how impedance information can be obtained from the wavelet transform. Comparison is made with data obtained from an LP measurement.

In the second part, a new EN analysis technique for computing impedance phase information from EN data will be briefly described and an example of its application given. The spectral noise impedance has a shortcoming in that it provides magnitude information only. The proposed analysis allows phase information to be obtained from the EN data.

II. WAVELET ANALYSIS

In this section, a set of ECN data is obtained from a non-stationary system. For illustration, the wavelet transform is applied to the data. A second series of measurements are taken on systems exhibiting different corrosion rates. Impedance information is obtained from the wavelet transform data and is compared with results from LP measurements.

The first, non-stationary system, consisted of a pair of 3 cm^2 mild steel cylindrical electrodes immersed in a 3% sodium chloride (brine) solution held at 60 °C. The electrodes were rotated at 1000 rpm in order to yield uniform corrosion patterns and to aid in diffusion of chemical species between the electrodes and bulk solution. The current flowing between the two electrodes was logged at a rate of 40 samples per second using a Zero Resistance Ammeter manufactured by ACM instruments.

Initially, the rate of corrosion was accelerated by bubbling CO_2, a corrosively aggressive gas, through the brine solution. After 6 hours, the CO_2 bubbling was ceased and replaced by N_2 bubbling. By doing so, the CO_2 was gradually displaced by N_2. It is expected that the N_2, being an inert gas, therefore resulted in a gradual decrease in the rate of corrosion.

0-7803-7218-2/02/$10.00 ©2002 IEEE

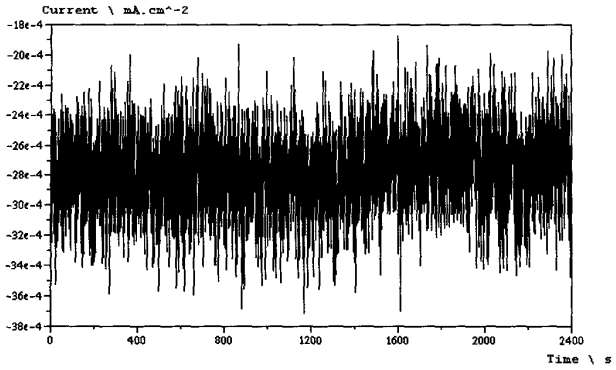

Fig. 1. ECN data logged during the period of accelerated corrosion due to dissolved CO_2.

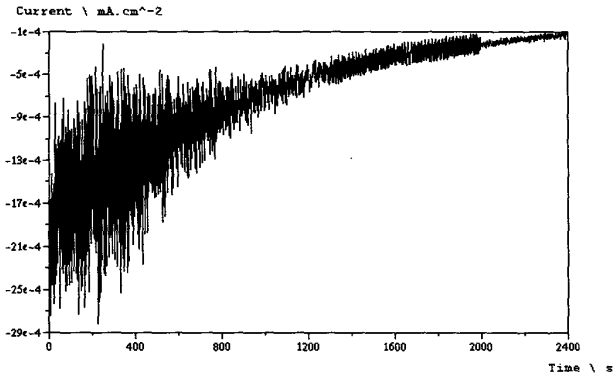

Fig. 2. ECN data logged upon commencement of N_2 bubbling.

The ECN was logged prior to, during and subsequent to the displacement of dissolved CO_2 gas by N_2 gas. Figs. 1 to 3 show the ECN signals obtained.

The wavelet transforms of the data shown in Figs. 1 to 3 are depicted in Figs. 4 to 6. They were obtained using the freely available and open source Scilab software [12] with the Fraclab toolbox [13].

The response to the decreased levels of dissolved CO_2 is clearly visible from the time plots. There is a general decrease in the magnitude of the ECN. This is also reflected in the wavelet transforms.

In Fig. 4, the wavelet transform has a large magnitude. In Fig. 5, the magnitude is seen to decrease gradually. In Fig. 6, after the system has reached an equilibrium, the magnitude is seen to be small in comparison with that of Fig. 4.

Thus the changes in the ECN signal due to a decrease in rate of corrosion has resulted in a general decrease in the magnitude of the wavelet transform.

To illustrate a quantitative application of the wavelet transform,

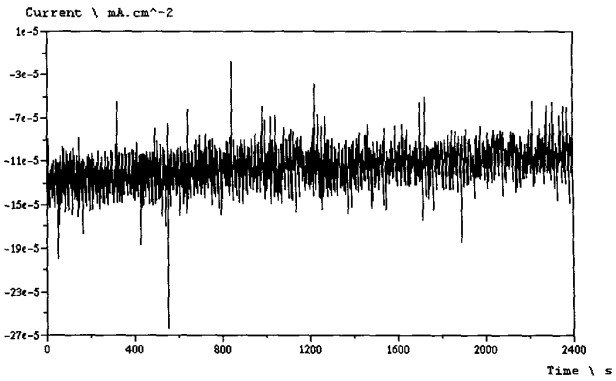

Fig. 3. ECN data logged during the period of low corrosion rate due to displacement of dissolved CO_2 by N_2.

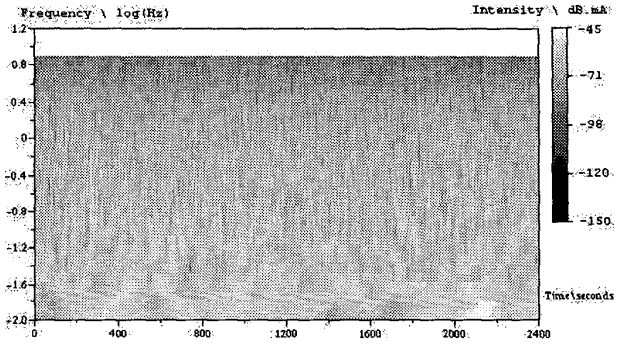

Fig. 4. Continuous wavelet transform of ECN data logged during the period of accelerated corrosion due to dissolved CO_2.

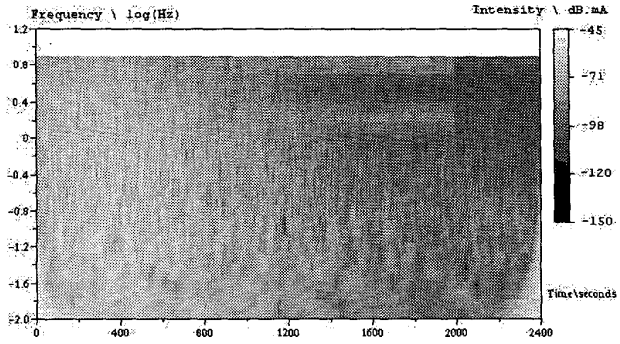

Fig. 5. Continuous wavelet transform of ECN data logged upon commencement of N_2 bubbling.

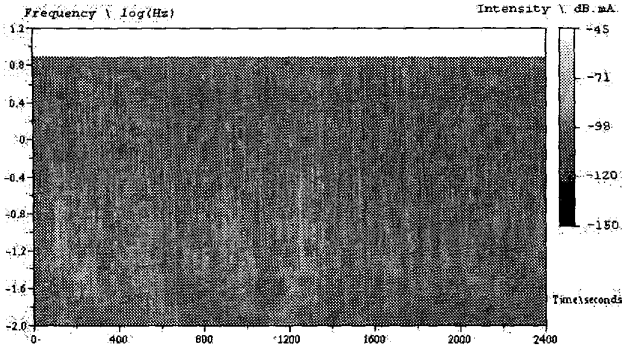

Fig. 6. Continuous wavelet transform of ECN data logged during the period of low corrosion rate due to displacement of dissolved CO_2 by N_2.

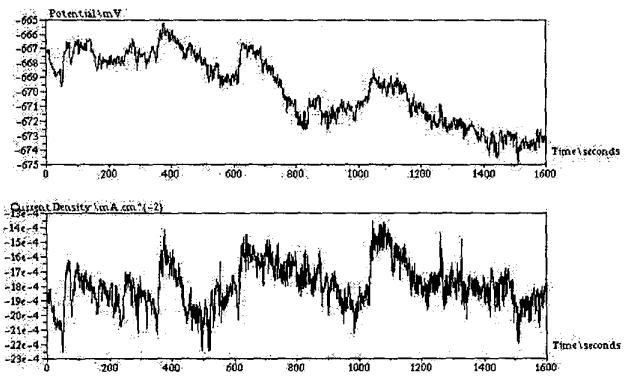

Fig. 7. EPN and ECN from non-rotating electrodes in inhibited solution

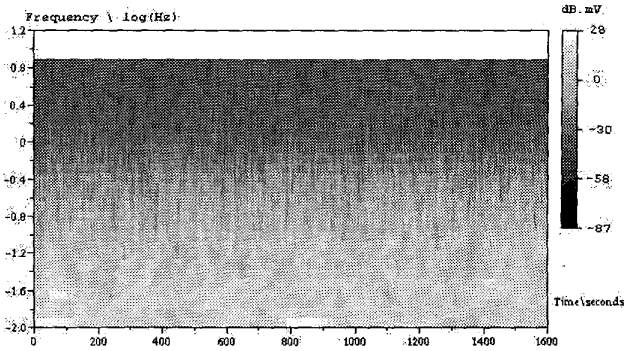

Fig. 8. Continuous wavelet transform power of EPN data from Fig. 7

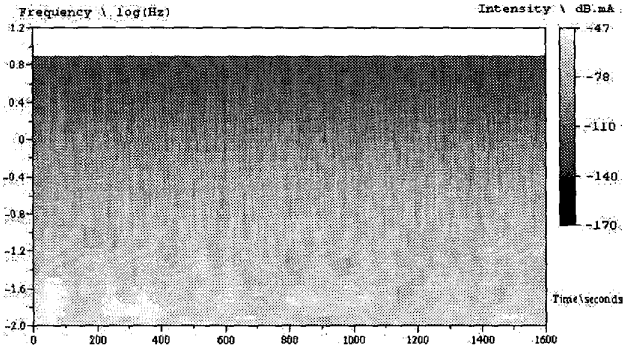

Fig. 9. Continuous wavelet transform power of ECN data from Fig. 7

an additional set of EN data was obtained from a set of stationary systems with different rates of corrosion. Linear polarization (LP) measurements were taken before and after each EN measurement in order to assess the rate of corrosion. The dual working electrode system of Eden *et al* [2] was used to obtain a simultaneous EPN/ECN measurement.

Four systems were studied: (i) electrodes were rotated at 1000 rpm in uninhibited 3% NaCl solution; (ii) non-rotating electrodes in uninhibited 3% NaCl solution; (iii) 1000 rpm rotation in 3% NaCl solution with 40 ppm of an organic inhibitor; (iv) non-rotating electrodes in the inhibited solution.

Figs. 7 to 9 show an example set of time plots and continuous wavelet transforms of the EN data obtained for non-rotating electrodes in the inhibited solution.

Figs. 8 to 9 show that the EN is dominated by low frequency (*ie* large scale) components. Since it is usually the low frequency information that is useful for noise impedance computations, a rough estimate of noise impedance can be obtained from the wavelet transform diagrams by comparing the maximum values in Figs. 8 and 9.

The maximum values are respectively 28 dB(mV) and -47 dB(mA.cm^{-2}). Thus the impedance modulus at low frequency is approximately 5.6 kΩ.cm^2. The LP measurements indicate an impedance of between 4.5 kΩ.cm^2 and 7.5 kΩ.cm^2, which agrees with the impedance obtained from the wavelet transform.

Table I compares the impedances obtained using LP with the impedances obtained from the wavelet transform diagrams. While there is some discrepancy between the two methods in some cases, there is generally good correlation. Both methods reflect the fact that the non-rotating electrodes have higher impedance (and thus lower rate of corrosion) than rotating electrodes and that the uninhibited solution gives rise to a lower impedance (*ie* higher rate of corrosion) than does the inhibited solution.

III. NYQUIST IMPEDANCE DIAGRAMS

Fig. 10 shows the equivalent circuit of the simultaneous EPN and ECN measurement described by Eden *et al* [2].

In Fig. 10, $Z_1(f)$ and $Z_2(f)$ are the electrochemical equivalent impedances of the two electrodes, $v_1(t)$ and $v_2(t)$ are the Thevenin equivalent EN sources associated with each electrode and $v(t)$ and $i(t)$ are the measured EPN and ECN respectively.

Measurement	LP (Ω.cm^2)	WT (Ω.cm^2)
1000 rpm, uninhibited	90	180
	90	250
1000 rpm, inhibited	600	560
0 rpm, uninhibited	450 to 570	450
	810	1780
0 rpm, inhibited	6000 to 7500	5000
	4500 to 7500	7000
	4500 to 10500	7000

TABLE I
IMPEDANCES OBTAINED BY LINEAR POLARIZATION (LP) AND FROM WAVELET TRANSFORM (WT) DIAGRAMS

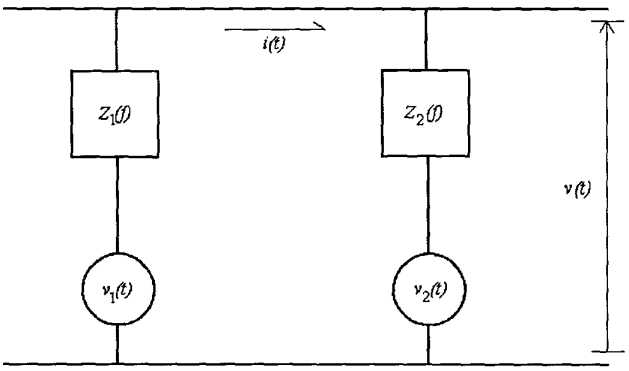

Fig. 10. Equivalent circuit of a simultaneous EPN and ECN measurement.

Bertocci *et al* [3] define the spectral noise impedance as

$$R_{\mathrm{sn}}(f) = \sqrt{\frac{S_{\mathrm{v}}(f)}{S_{\mathrm{i}}(f)}} \tag{1}$$

where $S_{\mathrm{v}}(f)$ is the power spectral density of the EPN and $S_{\mathrm{i}}(f)$ is the power spectral density of the ECN.

For identical impedances of $Z_1(f) = Z_2(f) = Z(f)$, the spectral noise impedance can be expressed as

$$R_{\mathrm{sn}}(f) = |Z(f)|\,. \tag{2}$$

Thus the spectral noise impedance can be used for measurement of the magnitude of the equivalent impedance of the electrodes.

A short coming of the spectral noise impedance method is that only the magnitude of the electrode impedance is discovered. The phase information is missing. This makes analysis more difficult as the precise topology of the impedance under investigation cannot be inferred with as much certainty.

In this paper, it is proposed that a newly defined quantity, the complex noise impedance,

$$Z_{\mathrm{sn}}(f) = \mathrm{E}\left[\frac{V(f)}{I(f)}\right] \tag{3}$$

can be used to extract the phase component of the impedance, given certain conditions regarding the symmetry of the electrode pair. In (3), $V(f)$ and $I(f)$ are the respective Fourier transforms of $v(t)$ and $i(t)$, and the E operator denotes statistical expectation.

By circuit analysis of Fig. 10 the complex noise impedance is found to be given by

$$\begin{aligned} Z_{\mathrm{sn}}(f) &= \mathrm{E}\left[\tfrac{V_2(f)}{V_1(f)-V_2(f)}\right] Z_1(f) + \mathrm{E}\left[\tfrac{V_1(f)}{V_1(f)-V_2(f)}\right] Z_2(f) \\ &= \alpha(f) Z_1(f) + \beta(f) Z_2(f) \end{aligned} \tag{4}$$

where $\alpha(f)$ and $\beta(f)$ are statistical properties relating to the EPN sources, $V_1(f)$ and $V_2(f)$, defined as implied by (4). It is usual to assume that the two EPN sources, $v_1(t)$ and $v_2(t)$, are statistically independent [3]. In that case, it is found that the $\alpha(f)$ and $\beta(f)$ terms are entirely real valued. Thus the phase of the complex noise impedance depends entirely on the phase of a weighted sum of the two electrode impedances.

In the case when $v_1(t)$ and $v_2(t)$ are known to be correlated, $\alpha(f)$ and $\beta(f)$ are complex valued and knowledge of the degree of correlation is required before any further use can be made of (4). The following assumes zero correlation between $v_1(t)$ and $v_2(t)$.

When the two electrode have identical impedances of $Z_1(f) = Z_2(f) = Z(f)$, (4) reduces to

$$Z_{\mathrm{sn}}(f) = k \cdot Z(f) \tag{5}$$

where

$$k = \mathrm{E}\left[\left|\frac{V_1(f)}{V_1(f) - V_2(f)}\right|^2\right] - \mathrm{E}\left[\left|\frac{V_2(f)}{V_1(f) - V_2(f)}\right|^2\right]. \tag{6}$$

In this case, $Z_{\mathrm{sn}}(f)$ is proportional to $Z(f)$. The constant of proportionality, k, is entirely real valued with either a zero, positive or negative value. As long as k is non-zero, the phase of $Z_{\mathrm{sn}}(f)$, is therefore equal to the phase of the impedances with possibly 180 ° (π radians) inversion depending on the sign of k.

However, k becomes zero when the electrodes have identical source EN characteristics as well as identical impedances. This enforces an important restriction on the technique: in order to extract the phase of the impedance, some asymmetry must exist between the two electrodes. The more asymmetric the electrodes become, the easier it is to extract the phase information.

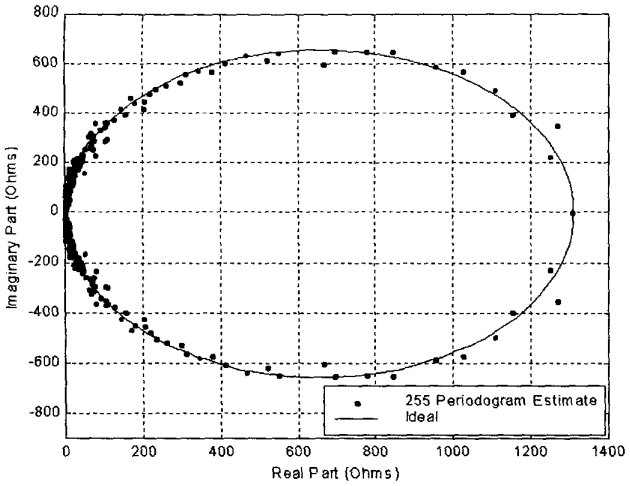

Fig. 11. Nyquist impedance diagram obtained from simulated EN with asymmetric potential sources

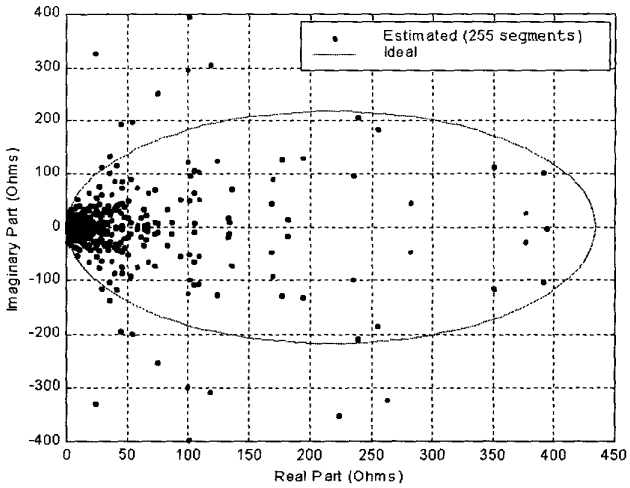

Fig. 12. Nyquist impedance diagram obtained from simulated EN with symmetric electrodes.

Fig. 11 shows the Nyquist impedance diagram obtained from a computer simulation of an electrode pair with identical impedances but different source EN powers. The impedance magnitude was computed by estimating $R_{sn}(f)$ in (1) and the phase was computed from an estimate of $Z_{sn}(f)$ in (3).

The figure shows good correlation between the estimated impedance and the expected impedance.

Fig. 12 shows the result of a computer simulation for an electrode pair with identical source EN and identical impedances. In this case, while the general magnitude of the impedance is approximately correct, the phase information is scattered randomly and there is very little correlation between the estimated and expected impedances. This is an example of where the proposed technique of phase recovery fails due to symmetric electrodes. From (6), $Z_{sn}(f)$ is zero for symmetric electrodes and the phase of zero is undefined.

Fig. 13 shows an example Nyquist impedance diagram computed using (3) to extract phase information and (1) for the magnitude. The EPN and ECN data was obtained from a physical system consisting of a pair of mild steel electrodes immersed in a NaCl solution with $NaNO_3$ added as a corrosion inhibitor. Significant crevice corrosion was observed on one of the mild steel electrodes whereas the other electrode remained free of visible corrosion. Based on these observations, it is concluded that the electrodes exhibited asymmetric impedances and EN power.

The approximately circular shape seen in Fig. 13 is typical of a parallel resistor/capacitor combination. It is thus inferred that the equivalent impedance of the electrode under investigation can be approximately modeled by a parallel resistor/capacitor. The value of the resistance is estimated from Fig. 13 to be approximately 100 $k\Omega.cm^2$. Such a large resistance is indicative of a low rate of corrosion.

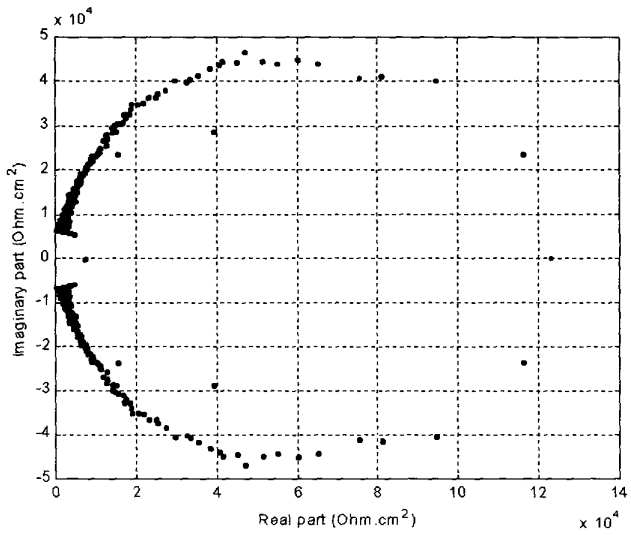

Fig. 13. Nyquist impedance diagram obtained from EN data.

IV. CONCLUSION

An example of a continuous wavelet transform has been given for analysis of electrochemical noise data. It is seen to be a useful technique for analysis of non-stationary systems. Impedance data obtained from the wavelet transform has been compared with linear polarization measurements.

The complex noise impedance has been described as a compliment to the conventional spectral noise impedance calculation. It has been shown, with supporting example, that if there is

some degree of asymmetry in the electrode pair, information regarding the phase of the equivalent impedances can be extracted.

The continuous wavelet transform and the complex noise impedance are two examples of the signal processing that can be applied to electrochemical noise data.

REFERENCES

[1] J. L. Dawson, "Electrochemical noise measurement: The definitive in-situ technique for corrosion applications?," in *Electrochemical Noise Measurement for Corrosion Applications*, Jeffery R. Kearns, John R. Scully, Pierre R. Roberge, David L. Reichert, and John L. Dawson, Eds. American Society for Testing and Materials, 1996, ASTM STP 1277, p. 3.

[2] D. A. Eden, K. Hladky, D. G. John, and J. L. Dawson, "Electrochemical noise — simultaneous monitoring of potential and current noise signals from corroding electrodes," in *Proceedings of Corrosion 86*. National Association of Corrosion Engineers, 1986.

[3] U. Bertocci, F. Huet, and M. Keddam, "Noise resistance applied to corrosion measurements i. theoretical analysis," *Journal of the Electrochemical Society*, vol. 144, no. 1, pp. 31–37, 1997.

[4] A. M. Lowe, H. Eren, Y. J. Tan, S. I. Bailey, and B. J. Kinsella, "Continuous corrosion rate measurement by noise resistance calculation," *IEEE Transactions on Instrumentation and Measurement*, vol. 50, no. 5, pp. 1059–1065, 2001.

[5] H. Xiao and F. Mansfeld, "Evaluation of coating degradation with electrochemical impedance spectroscopy and electrochemical noise analysis," *J. Electrochem. Soc.*, vol. 141, no. 9, pp. 2332, 1994.

[6] U. Bertocci, F. Huet, B. Jaoul, and P. Rousseau, "Noise resistance applied to corrosion measurements ii. experimental tests," *Journal of the Electrochemical Society*, vol. 144, no. 1, pp. 37–43, 1997.

[7] F. Mansfeld, L. T. Hans, C. C. Lee, and G. Zhang, "Evaluation of corrosion protection by polymer coatings using electrochemical impedance spectrscopy and noise analysis," *Electrochemica Acta*, vol. 43, pp. 2933–2945, 1998.

[8] F. Mansfeld, "Electrochemical impedance spectrscopy (eis) as a new tool for investigation methods of corrosion protection," *Electrochmica Acta*, vol. 35, no. 10, pp. 1533–1544, 1990.

[9] Y. J. Tan, S. Bailey, B. Kinsella, and A. Lowe, "Mapping corrosion kinetics using the wire beam electrode in conjunction with electrochemical noise resistance measurements," *J. Electrochem. Soc.*, vol. 147, no. 2, pp. 530–539, 2000.

[10] American Society for Testing and Materials, West Conshohocken, PA, *Standard Practice for Conducting Potentiodynamic Polarization Resistance Measurements*, 1997.

[11] X. D. Dai, *Wavelet Applications in Process Sensor Data Analysis*, Ph.D. thesis, Washington University Sever Institute of Technology, 1996.

[12] INRIA-Rocquencourt, "Scilab," http://www.rocq.inria.fr /scilab, 2002.

[13] INRIA-Rocquencourt, "Fraclab," http://www-rocq.inria.fr /fractales/fractales-eng.html, 2002.